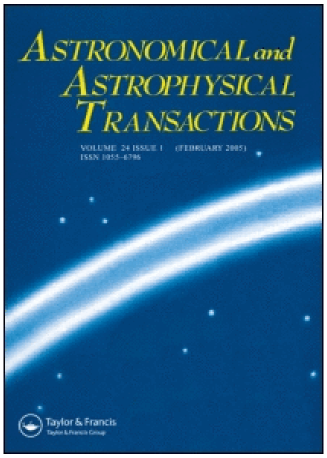

Astronomical & Astrophysical Transactions
The Journal of the Eurasian Astronomical Society
Publication details, including instructions for authors and subscription information:
http://www.informaworld.com/smpp/title~content=t713453505

Using pulsar scintillation to probe AU-size structure in the interstellar medium

D. Stinebring [a]
[a] Department of Physics and Astronomy, Oberlin College, Oberlin, OH, USA

Online Publication Date: 01 December 2007
To cite this Article: Stinebring, D. (2007) 'Using pulsar scintillation to probe AU-size structure in the interstellar medium', Astronomical & Astrophysical Transactions, 26:6, 517 - 524
To link to this article: DOI: 10.1080/10556790701614862
URL: http://dx.doi.org/10.1080/10556790701614862

Astronomical and Astrophysical Transactions
Vol. 26, No. 6, December 2007, 517–524

Using pulsar scintillation to probe AU-size structure in the interstellar medium

D. STINEBRING*

Department of Physics and Astronomy, Oberlin College, Oberlin, OH 44074, USA

(Received 19 July 2007)

It is well known that pulsar dynamic spectra occasionally show pronounced fringing or criss-cross patterns. It was a surprise, however, that a two-dimensional Fourier analysis of these spectra showed faint, parabolic features, which are now called scintillation arcs. I will show evidence that the scintillation arc phenomenon is widespread and that it underpins many other scintillation phenomena. If an estimate of the distance to the pulsar and a measurement of its proper motion exist, then the location of the scattering material along the line of sight can be determined. There is often pronounced substructure in the arcs, and it translates along the main arc in a manner that is determined by the proper motion of the pulsar. This substructure may be produced by lens-like features in the ionized interstellar medium that are far out of pressure balance with the warm ionized medium and that may be related to deterministic structures that cause extreme scattering events. Observations with this technique, which rely on a large flux density and/or a large collecting area, have an angular resolution of about a milliarcsecond. They often show features in the scatter broadened image out to 15–20 times this resolution. Thus, single-dish observations can study details in the scattering medium on AU-size scales while covering a relatively large field of view that scans the sky at the pulsar proper motion speed. We are still learning how to interpret the richly detailed scintillation arc pattern that results, and observational and interpretive surprises continue to emerge.

Keywords: Scintillation arcs; Interstellar medium; Pulsar scintillation

1. Introduction

The subject of this conference is scattering and scintillation in radio astronomy. Pulsars have been an important part of that investigation for many years. In fact, we owe the discovery of pulsars to the effort to understand the scintillation of radio sources in the interplanetary medium and the perspicacity of Hewish *et al.* [1]. Pulsars have turned out to be nearly ideal sources to investigate interstellar scintillation (ISS) since they are so compact, since nearly 1800 of them are now known, and since we have methods to determine the distance to them. Reviews of pulsar scintillation have been written by Rickett [2], Hewish [3], and Narayan [4], but many developments have occurred since those reviews were prepared.

*Email: dan.stinebring@oberlin.edu

Astronomical and Astrophysical Transactions
ISSN 1055-6796 print/ISSN 1476-3540 online © 2007 Taylor & Francis
http://www.tandf.co.uk/journals
DOI: 10.1080/10556790701614862

Focus of this review is the phenomenon of *scintillation arcs*, which are faint but distinct patterns in the Fourier analysis of pulsar dynamic spectra. Rickett (in these Proceedings) introduces the background material needed to understand ISS, in general, and scintillation arcs, in particular.

Briefly, multi-path scattering in the interstellar medium (ISM) of the spatially coherent radiation from pulsars causes an interference pattern at the observer. This is called the dynamic spectrum and is a measure of the flux density of the source as a function of radio frequency and time, $S_1(\nu, t)$. The interference is a deeply modulated random signal in the dynamic spectrum plane, exhibiting exponential fluctuation statistics over this plane because of the Gaussian fluctuations of the two components of the E-field for each polarization. This random signal exhibits interference maxima called 'scintiles' that have size ν_d and t_d in the $S_1(\nu, t)$ plane. The power spectrum of the dynamic spectrum, often denoted $S_2(f_\nu, f_t)$ and called the secondary spectrum (SS), presents the fluctuation power in the dynamic spectrum. Since the input signal is real, $S_2(-f_\nu, -f_t) = S_2(f_\nu, f_t)$.

Additional, non-random features had been noted in dynamic spectra for many years. These included periodic fringe patterns and the occasional presence of a criss-cross pattern in the dynamic spectrum [5–10]. These were generally attributed to strong refractive effects in the medium that occasionally split the image (*i.e.* the brightness distribution on the sky) into multiple parts, shifted the centroid of the image substantially away from the pulsar position, or both. But, this seemed puzzling because there was significant evidence that the ISM fluctuations basically followed a Kolmogorov spectrum [11, 12]. A Kolmogorov turbulence spectrum does not have enough bending power on large spatial scales to produce effects such as these [10].

After the upgraded Arecibo telescope came back into operation in 1999, we started making dynamic spectrum observations with the new instrument. Although most of the work at the time focused on the two-dimensional (2-D) autocorrelation of the dynamic spectrum, we tried

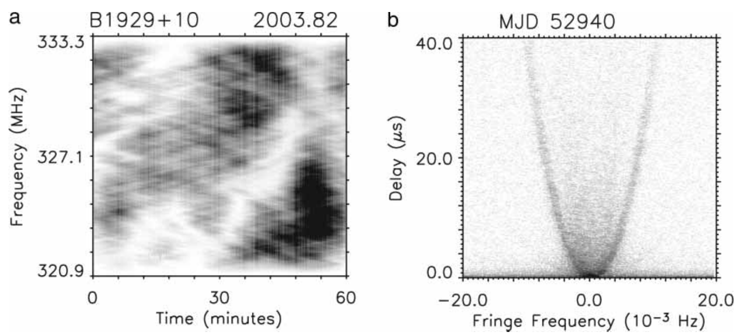

Figure 1. (Left) A dynamic spectrum for the pulsar PSR B1929 + 10 recorded at the Arecibo Observatory. Flux density is displayed with a linear grayscale with black representing the strongest power. In addition to the large-scale power (normal diffractive scintillation), there is a low-level criss-cross pattern visible across the frame. (Right) The SS, which is simply the 2-D power spectrum of the dynamic spectrum. Only the upper half-plane is shown because the lower half-plane is redundant since the input signal (the dynamic spectrum) is real. Spectral power is displayed logarithmically, and the dynamic range displayed (maximum near the origin to the rms noise level) is more than a factor of 10^5. The conjugate radio frequency axis, which conventionally would have been labeled cycles per MHz, has been relabeled *delay* because it represents the differential delay between non-central ray paths and the center of the image. Similarly, the conjugate time axis, which conventionally would be labeled cycles per second is relabeled *fringe frequency* because it can be interpreted as the temporal fringe frequency caused by rays beating with the central portion of the image. The horizontal axis can also be calibrated in terms of the angular offset of rays from the location of the pulsar. In this case, the conversion factor is 20 mHz = 8.3 mas with a screen location determined to be $s = 0.40$. This underscores the remarkable resolving power coupled with the wide 'field of view' inherent in scintillation arc analysis.

a Fourier analysis on the data. We were motivated in this by Cordes and Wolszczan's [8, 9] pioneering work and by Rickett *et al.* [13] startling report of 'fringing' (*i.e.* a periodic 2-D sinusoid of low-level power in the dynamic spectrum) for the pulsar PSR B0834 + 06. In addition to power near the origin of the SS due to standard diffractive scintillation, we were seen faint hints of power extending outward along a curving path. We were concerned initially about the reality of this signal, but we slowly developed confidence that it was due to scattering in the ISM [14]. We reported the discovery of what are now called scintillation arcs [15] in 2001. An example of the phenomenon is shown in figure 1.

2. Basic theory

Theory of scintillation arcs has been presented in detail in the last several years [16, 17]. I follow the notation and approach of Cordes *et al.* (hereafter CRSC) below. Since there is observational evidence in scintillation arc data that a substantial amount of scattering takes place in one or more thin screens along the line of sight, we specialize our treatment to that case. Consider the radiation to be propagating along the z-axis and locate the pulsar at $z = 0$, the observer at $z = D$, and the scattering screen at $z = sD$, where $0 \leq s \leq 1$ parameterizes the screen location. Denoting the electromagnetic phase at the observer plane ($z = D$) by Φ, it can be expanded around the center of the observing window (ν_0, t_0) in the following fashion:

$$e\Phi \approx \Phi_0 + 2\pi(f_t \delta t + f_\nu \delta\nu), \tag{1}$$

where $f_t = (1/2\pi)\partial_t \Phi$ is the differential Doppler shift and $f_\nu = (1/2\pi)\partial_\nu \Phi$ is the differential group delay. Neglecting dispersive delays in the phase screen, which seems warranted based on the observations, the fringe frequencies for rays coming from θ_1 and θ_2 (measured relative to the pulsar position at the origin) are

$$f_\nu = \left[\frac{D(1-s)}{2cs}\right]\left(\theta_1^2 - \theta_2^2\right), \tag{2}$$

$$f_t = \left(\frac{1}{\lambda s}\right)(\theta_1 - \theta_2) \cdot V_\perp. \tag{3}$$

Here, λ is the wavelength at the center of the band, and $V_\perp$ is the velocity of the point in the screen intersected by a straight line from the pulsar to the observer, given by a weighted sum of the velocities of the source, screen and observer [18]:

$$V_\perp = (1-s)V_{p\perp} + sV_{\text{obs}\perp} - V_{\text{screen}\perp}. \tag{4}$$

CRSC demonstrate that the power distribution in the SS is a distorted autocorrelation of the scatter-broadened image on the sky using equations (2) and (3) for the mapping from image coordinates to the SS plane. There are at least two situations in which the scatter-broadened image on the sky is dominated by a central 'core' that is small compared with the rest of the image: (1) in the case of weak scattering, when there is a true unscattered core, and (2) in the case of strong scattering (the usual situation for meter wavelength observations of pulsars) when the inhomogeneity spectrum is shallow enough (*e.g.* like that produced by Kolmogorov turbulence) so that the image has a quasi-Gaussian core and an extended halo of weaker intensity (see CRSC for more details). In either situation, we can set $\theta_2 = 0$ as an approximation. This condition and the localization of the scattering in a thin screen are essential to the production of a well-defined parabolic scintillation arc. Choosing the x-axis to be along the weighted velocity vector [equation (4)] and considering interference between rays from the image (θ_x, θ_y) and the central point of the image, we have a parabola in the $S_2(f_\nu, f_t)$ plane: $f_\nu = af_t^2 + b$, where

$$a = \frac{s(1-s)D\lambda^2}{2cV^2}, \quad b = \frac{D(1-s)\theta_y^2}{2cs}. \tag{5}$$

Since b is positive-definite, the parabola with $b = 0$ will define an outer boundary to the power distribution in the most idealized case. Remarkably, something approximating this idealized case occurs frequently in practice, resulting in sharply defined parabolas in S_2. This contains important clues about the distribution of material in the ISM and, as Rickett has emphasized in these Proceedings, the anisotropy of the scattering.

Since in many cases the curvature of the parabola can be measured with a good deal of precision, it is possible to use the expression for a and independent information about the pulsar distance and its proper motion to determine the location of the scattering material along the line of sight [19]. (Many of the strong pulsars for which scintillation arc observations are possible also have well-measured proper motions and, in some cases, parallax distances, as well.) Although it would appear from the form of the curvature value a that there is a two-fold degeneracy in the determination of distance to the screen, but this is not a problem in practice. In many cases, the pulsar velocity so dominates the terms in equation (4) that the curvature constant becomes

$$a_{\mathrm{psr}} = \frac{sD\lambda^2}{2c(1-s)^2V_p^2}, \tag{6}$$

which is monotonically increasing over the range $0 \leq s \leq 1$. (In this expression, V_p is the pulsar's transverse velocity.) Even when the Earth's motion is non-negligible compared with the motion of the pulsar, equation (5) can be used with observations taken over a year to determine the screen location uniquely. An example of this latter case is presented by Stinebring [20]. No one has used careful observations of low-velocity pulsars over the course of a year to try and put a limit on the screen velocity using equation (5), but this should be possible, in principle.

In the best cases – when the core dominates the image – the SS contains an invertible map of the sky brightness in the S_2 plane. In other cases, particularly when there is a discrete substructure in the SS, it is clear that cross-terms between N discrete image components are giving rise to $\sim N(N-1)/2$ features in the SS. Motivated by this, Walker and Stinebring [21] developed an iterative technique, akin to CLEAN, that identifies the fundamental components of the image as it accounts for all the power in the SS. This shows promise in converting secondary spectra (obtained with single-dish observations) into images of the sky with milliarcsecond resolution and tens of milliarcsecond field of view, but see Trang and Rickett [22] for some caveats and the development of another approach.

3. Observational overview

Updating the observational overview in CRSC, we summarize the major properties of scintillation arc observations.

1. Scintillation arcs are faint, but they are ubiquitous. Of 12 bright ($S_{400} > 60$ mJ year) pulsars that we have observed at Arecibo, 10 display scintillation arcs, and the other two have

features related to arcs. In an effort to assess the frequency of occurrence of scintillation arcs, Minter, Ransom (NRAO), and I observed 18 pulsars with the NRAO/GBT. The sources were selected to have $DM < 50\,\mathrm{pc\,cm^{-3}}$ and $S_{400} > 20$ mJ year. We detected scintillation arcs toward 16 out of the 18 pulsars in this sample [23].

2. The arcs often have a sharp outer edge, particularly at radio frequencies above >1 GHz, but there are also many instances of diffuse parabolic power distributions. At least in some cases, the same pulsar exhibits a scintillation arc that is sharply defined at some epochs and diffuse at others (see figure 2).
3. The arc outlines are parabolic with minimal tilt or offset from the origin: $f_\nu = af_t^2$, but see Trang and Rickett [22] for a more detailed analysis in one case.
4. The power distribution along the arc can highly be asymmetric in f_t for a given f_ν, can show significant substructure, and can change dramatically as a function of time. Two examples are shown in figures 3 and 4.
5. A particularly striking form of substructure consists of inverted 'arclets' with the same value of $|a|$ and with apexes that lie along or inside the main arc outline. See CRSC [16] and Walker *et al.* [17] for details and Hill *et al.* [24] for a remarkable example.
6. Although a single scintillation arc is usually present for each pulsar, there are now six cases in which multiple scintillation arcs (with different a values) are seen [19]. For the very bright pulsar PSR B1133 + 16, four distinct a values have persisted for more than 25 years for observation.
7. Arc curvature accurately follows a simple scaling law with radio frequency [25]: $a \propto \nu^{-2}$. The scintillation arc structure is often traceable from ~300 to 1400 MHz or higher, indicating that the phenomenon is not fundamentally related to the transition from weak to strong scintillation (because the scintillation strength is a strong function of frequency).
8. The arc curvature parameter a is constant at the 5–10% level for ~20 years for the half dozen pulsars for which we have long-term data spans.

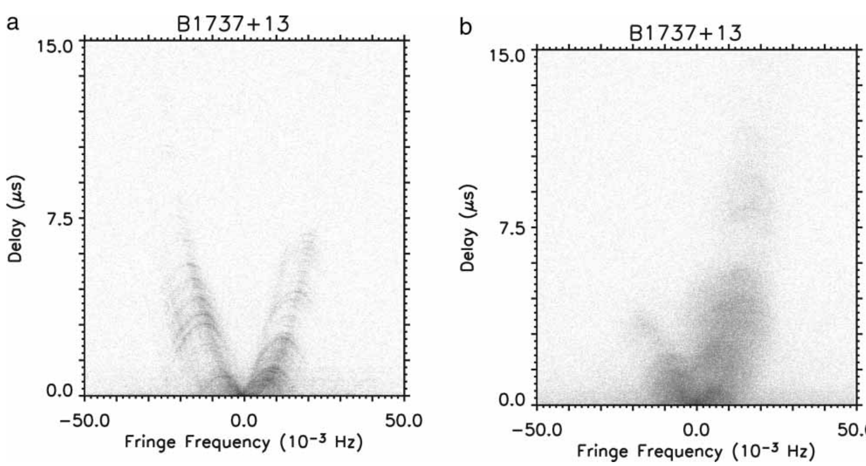

Figure 2. Two secondary spectra of PSR B1737 + 13 taken about four months apart, both at the Arecibo Observatory at 1425 MHz using a 50 MHz bandwidth. Details of the secondary spectra are similar to those in figure 1. (Left) An observation made on 27 May 2006 (MJD = 53882) that shows sharply defined arclet features across a broad locus of parabolic power. (Right) An observation made on 19 September 2006 (MJD = 53997) in which the sharp structure has been blurred out by extra scattering. These are drawn from a set of 36 weekly observations and are representative of the larger sample. The transition from sharply defined arclets to a diffuse power distribution occurred over a several week period around MJD 53904.

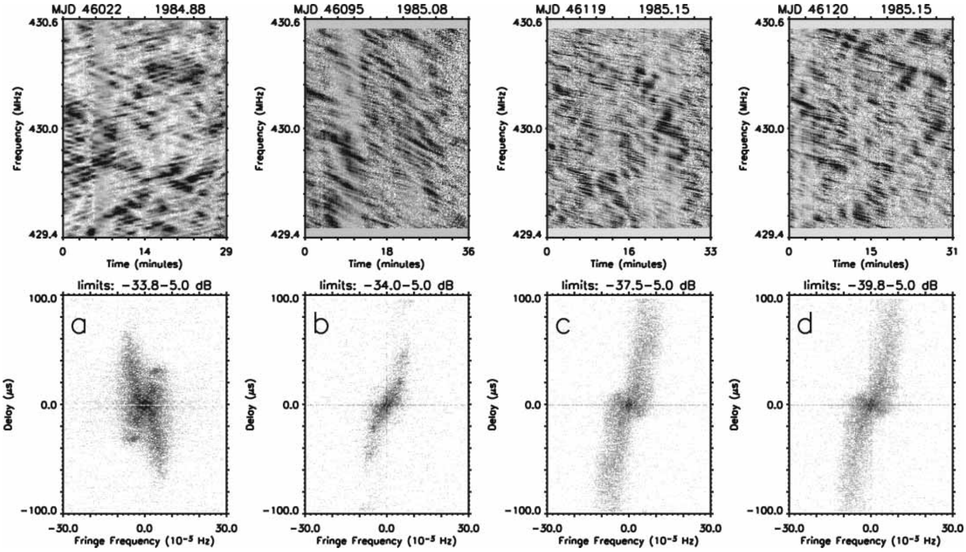

Figure 3. Dynamic (upper row) and secondary spectra for pulsar PSR B0919 + 06 taken with the Arecibo telescope by J. M. Cordes. Note that the full SS plane is shown, with reflection symmetry through the origin. The blurring in some of the dynamic spectra is a processing artifact and does not affect the secondary spectra. At epoch a, a two-sided parabola is present although the power distribution is highly non-uniform. There is a localized region of SS power at the top of the arc in the first quadrant. Observation b, taken 73 days later, shows a completely one-sided parabola (referring to just the upper half-plane of the SS). The one-sided nature of the SS continues 24 and 25 days later at epochs c and d, respectively, and has become more extensive. Even higher spectral resolution would have been necessary to capture all the SS power. Although the dynamic spectra at these epochs would have been said to exhibit 'tilted scintles' in earlier classification schemes, a parabolic scintillation arc underlies this distribution. This is a general result: scintillation arcs are the most basic unit of power distribution in secondary spectra; asymmetries and substructure along the scintillation arc then determine the overall character of the dynamic spectrum distribution. The cause of these power asymmetries, which can change on the refractive timescale [11, 26], has not been determined.

4. Further questions

Although scintillation arcs provide a more detailed tool for understanding the distribution of inhomogeneities in physical and wavenumber space, there is a lot that we do not understand about the phenomenon, and hence about the ISM itself. In particular, we face these substantial puzzles or questions.

1. Why are scintillation arcs often sharply defined? This is puzzling because it implies not only a high degree of anisotropy in the image, but also a relatively close alignment between the velocity vector of the pulsar and the long axis of the scattered image. See CRSC for details and the recent paper by Trang and Rickett [22].
2. What are the astrophysical structures that cause arclet substructure in scintillation arcs?
3. What are the astrophysical structures that we should associate with the 'thin screens' that clearly exist along the line of sight to most pulsars?
4. What fraction of the column density of electrons along the line of sight is contributing to the scattering? We have very little firm data on this important question, and yet there is information in the SS that can help to answer it.
5. How much of the scattering takes place in the extended medium between the pulsar and the observer compared with the amount that takes place in (relatively) thin and distinct screens?

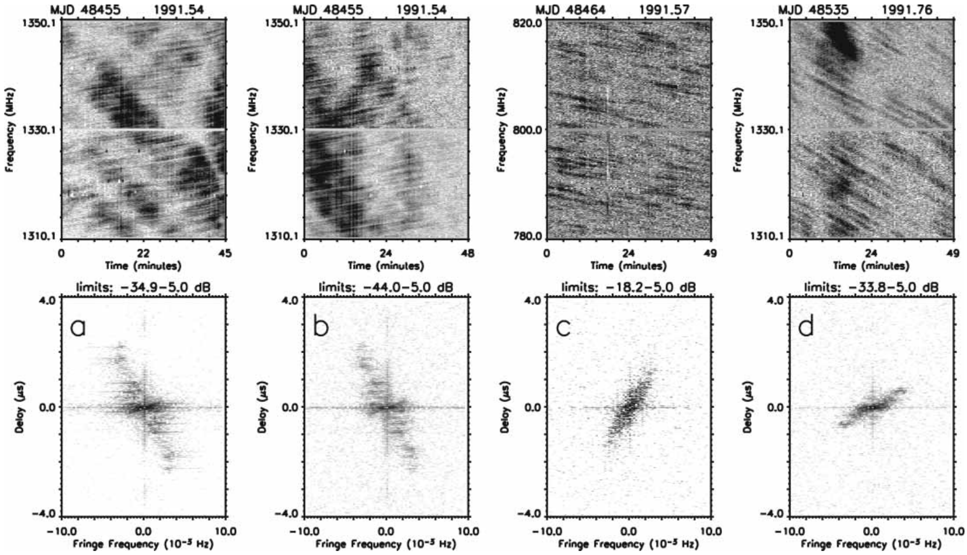

Figure 4. Dynamic and secondary spectra for pulsar PSR B0355 + 54 taken with the NRAO 42-m telescope over a 3-month period with R. Foster. Note that observation *c* is at a different frequency and it is *possible* that the fringe frequency axis is reversed; however, the fringe frequency axis at epoch *d* is oriented correctly. Observations *a* and *b* were taken in two consecutive hours and show that the SS does not change during that time despite the fact that the dynamic spectra are completely different in large-scale features. By epoch *d* the left–right symmetry of the scintillation pattern has reversed. An ensemble average of many observations of this pulsar shows a full scintillation arc that is parabolic in shape. As in figure 3, the tilted scintle phenomenon is seen to be a scintillation arc with asymmetric power distribution. The asymmetry of power in the S_2 plane has not been adequately explained, now that it does not appear to be due to large refractive features in the ISM.

5. Summary

Although several theoretical treatments of scintillation arcs now exist [16, 17] and observational details are emerging [15, 19, 24, 25], many fundamental questions remain unanswered. Most basically, we do not know what astrophysical entities are responsible for the scattering ‘screens’ that appear prominently along the line of sight to most pulsars. We do not understand the source of the power asymmetry in secondary spectra power distributions, and we do not understand the fine-scale substructure in secondary spectra that is often in the form of arclets.

Progress in this field requires new, well-focused observations as well as realistic simulations of radio wave scattering in the ISM. There is much room for creative thought and analysis since many high-quality observational clues exist. We need to go beyond our current conception of the ISM in order to identify the features responsible for the wealth of scintillation arc details.

Acknowledgements

I thank the organizers of this conference for the opportunity to discuss scintillation in such a congenial setting. This research was supported by grant no. AST-0407302 from the US National Science Foundation.

References

[1] A. Hewish, S.J. Bell, J.D.H. Pilkington *et al.*, Nature **217** 709 (1968).
[2] B.J. Rickett. Ann. Rev. Astr. Ap. **28** 561 (1990).

[3] A. Hewish. *Pulsars as Physics Laboratories*, vol. 151 (Oxford University Press, Oxford, 1993).
[4] R. Narayan. *Pulsars as Physics Laboratories*, vol. 167 (Oxford University Press, Oxford, 1993).
[5] M.S. Ewing, R.A. Batchelor, R.D. Friefeld *et al.*, Astrophys. J. **162** L169 (1970).
[6] J.A. Roberts and J.G. Ables, MNRAS **201** 1119 (1982).
[7] A. Hewish, A. Wolszczan and D.A. Graham, MNRAS **213** 167 (1985).
[8] J.M. Cordes and A. Wolszczan, Astrophys. J. **307** L27 (1986).
[9] A. Wolszczan and J.M. Cordes, Astrophys. J. **320** L35 (1987).
[10] B.J. Rickett, A.G. Lyne and Y. Gupta, MNRAS **287** 739 (1997).
[11] D.R. Stinebring, T.V. Smirnova, T.H. Hankins *et al.*, Astrophys. J. **539** 300 (2000).
[12] H.C. Lambert and B.J. Rickett, Astrophys. J. **531** 883 (2000).
[13] B.J. Rickett, A.G. Lyne and Y. Gupta, in *Pulsars: Problems and Progress, IAU Colloquium*, edited by S. Johnston, M.A. Walker and M. Bailes, vol. 160 (Astronomical Society of the Pacific, San Francisco, 1996), p. 471.
[14] D.R. Stinebring, in *Small Ionized and Neutral Structures*, edited by M. Goss, and M. Haverkorn. ASP Conference Series. **365** 254 (2007).
[15] D.R. Stinebring, M.A. McLaughlin, J.M. Cordes *et al.*, Astrophys. J. **549** L97 (2001).
[16] J.M.Cordes, B.J. Rickett, D.R. Stinebring *et al.*, Astrophys. J. **637** 346 (2006).
[17] M.A. Walker, D.B. Melrose, D.R. Stinebring *et al.*, MNRAS **354** 43 (2004).
[18] J.M. Cordes and B.J. Rickett, Astrophys. J. **507** 846 (1998).
[19] M.L. Putney and D.R. Stinebring, Chin. J. Astron. Astrophys. **6**(2) 233 (2006).
[20] D.R. Stinebring, Chin. J. Astron. Astrophys. **6**(2) 204 (2006).
[21] M.A. Walker and D.R. Stinebring, Mon. Not. R. Astron. Soc. **362** 1279 (2005).
[22] F.S. Trang and B.J. Rickett, Astrophys. J. **661** 1064 (2007).
[23] M.L. Putney, A.H. Minter, D.R. Stinebring *et al.*, In Bulletin of the American Astronomical Society, **37** 1470 (2005).
[24] A.S. Hill, D.R. Stinebring, C.T. Asplund *et al.*, **619** 171 (2005).
[25] A.S. Hill, D.R. Stinebring, H.A. Barnor *et al.*, Astrophys. J. **599** 457 (2003).
[26] B.J. Rickett, W.A. Coles and G. Bourgois, **134** 390 (1984).